NATIONAL ADVISORY COMMITTEE FOR AERONAUTICS

WARTIME REPORT

ORIGINALLY ISSUED
July 1942 as
Advance Confidential Report

CALIBRATIONS OF PITOT-STATIC TUBES AT HIGH SPEEDS

By Reece V. Hensley

Langley Memorial Aeronautical Laboratory
Langley Field, Va.

WASHINGTON

NATIONAL ADVISORY COMMITTEE FOR AERONAUTICS

ADVANCE CONFIDENTIAL REPORT

CALIBRATIONS OF PITOT-STATIC TUBES AT HIGH SPEEDS

By Reece V. Hensley

SUMMARY

Three types of service pitot-static tube were calibrated over an approximate range of speeds of 150 to 600 miles per hour. A standard Prandtl-type pitot-static tube was calibrated over the same speed range. These calibrations indicated the need for a pitot-static tube having greater accuracy, especially at high speeds. A high-speed pitot-static tube was therefore designed and calibrated over the same speed range. The characteristics of this pitot-static tube were found to be comparable with those of the standard Prandtl-type pitot-static tube at low speeds, but they were found to be considerably better than those of the Prandtl-type instrument at high speeds.

INTRODUCTION

At the request of the Bureau of Aeronautics, Navy Department, three types of standard service pitot-static tube were calibrated in the NACA 24-inch high-speed wind tunnel. The calibrations were made over an approximate range of speeds of 150 to 600 miles per hour.

Following the calibration of the standard service pitot-static tubes, check calibrations were made on several Prandtl-type pitot-static tubes that are used as standard laboratory instruments.

The results of these calibrations indicated the need for a pitot-static tube having a more rugged construction than the Prandtl type to reduce the possibility of changes in the calibration factor and for a design to make the calibration factor nearer unity and to maintain that factor with a minimum of variation over a large speed range.

A high-speed pitot-static tube was designed to attain this purpose. The design and calibration of this

instrument, together with the calibrations of the other pitot-static tubes are presented herein.

APPARATUS AND TESTS

Tunnel Calibrations

The 24-inch high-speed wind tunnel, in which these calibrations were made, is an induction-type wind tunnel without return passage, having its induction nozzle downstream from the test section. A detailed description is given in reference 1.

The impact, or total, pressure at the test section is equal to atmospheric pressure except for a small loss through screens. This loss, equal to approximately 0.13 percent of the dynamic pressure q, has been computed from measurements of the loss through screens and has been checked by comparison of the impact-pressure indications obtained with several standard pitot tubes.

The static pressure at the test section was determined by calibrated static-pressure orifices in the tunnel wall upstream from the test section. Calibrations of these orifices were made in the usual manner by comparing the static pressure at the orifices with the static pressure at the test section. The static pressure at the test section was determined for the calibrations by measurements of the pressure acting on orifices at the test-section level in a long tube that extended from the region of practically zero velocity ahead of the entrance cone to a point well downstream of the test section. Static-pressure tubes of two sizes, 1/8 inch and 3/4 inch in diameter, were used in these calibrations. Identical results were obtained with both tubes.

In order to simplify the calculations and to minimize the accidental errors involved, for the later tests the static pressure in the test section was measured simultaneously with the impact and static pressures indicated by the pitot-static tube, thereby eliminating the necessity for the use of the orifices in the tunnel wall upstream from the test section. This measurement was accomplished by installing the long 1/8-inch-diameter tube in the tunnel in addition to the pitot-static tube. The pressure at the static-pressure orifices was measured during a

number of these tests to determine any interference effects. The results indicated no appreciable change in the calibration of the static-pressure orifices with or without the pitot-static tube installed in the tunnel.

Pitot-Static Tubes

Service tubes.- The three types of service pitot-static tube calibrated are the following:

Kollsman Instrument Co. F.S.S.C. No. 18-T-4545 (fig. 1), designated tube 1

Aero Instrument Co. F.S.S.C. No. 18-T-4554 (fig. 2), designated tube 2

Aero Instrument Co. N.A.F. 39968. Bureau of Aeronautics drawing No. 548-SK (fig. 3), designated tube 3

Two instruments of each type, identified as a and b, were furnished by the Bureau of Aeronautics, Navy Department, and all instruments were calibrated.

Tubes 1 and 2 were mounted on a long support tube in the center of the tunnel. This tube, which had the same diameter as the pitot-static tube, formed a rearward extension of the pitot-static tube and was supported by two sets of three equally spaced wires fastened to the tunnel walls. The wires were located sufficiently far downstream from the static-pressure orifices of the instrument to insure that they would have no effect on the static-pressure indications of the instrument.

Tube 3 was mounted on the tunnel wall and the pressure leads passed through the wall. One instrument of this type was tested both with and without fairing; the fairing covered the mounting and pressure leads and was shaped to produce a smoother flow in the region of the instrument. The second instrument was tested only without the fairing.

Prandtl tube.- The Prandtl tube has the dimensions of a normal pitot-static tube of this type (reference 2). This instrument was mounted for calibration by passing the support tube through a hole in the tunnel wall and by fastening the support tube in the chamber surrounding the test section.

High-Speed tube.- In the design of the high-speed pitot-static tube (fig. 4) the static-pressure orifices were located in a region such that the static-pressure indications of the instrument at high velocities would be equal to the true static pressure. This location was determined from unpublished data obtained from tests in the NACA 11-inch high-speed wind tunnel of the pressure distribution along the axis of a pitot-static tube. Insufficient data being available to give the nose shape for minimum errors in the static-pressure indications, the tube was so designed that the nose could be removed; noses of four different shapes were calibrated. These four nose shapes (shown in figure 5) are A, hemispherical; B, semiellipsoidal, having a fineness ratio of 2:1; C, having ordinates given by the equation $y = 1.886\sqrt{x} - x + 0.083x^2$; and D, semiellipsoidal, having a fineness ratio of 4:1. The spindle of the high-speed pitot-static tube is a 2.8-inch-chord NACA 16-009 airfoil that is fitted to a specially constructed streamline support strut. The basic dimensions of this pitot-static tube are given in figure 4. This instrument was mounted in the tunnel in the same manner as the Prandtl-type pitot-static tube.

Scope of Tests

All the service instruments and the Prandtl-type standard instrument were calibrated only at an angle of attack of 0°. The high-speed pitot-static tube was calibrated through a range of angles about the axis of the support tube from 0° to 12°, in 4° increments. Each of the instruments was calibrated over an approximate range of speed of 150 to 600 miles per hour.

PRECISION

All measurements were made in such a manner that accidental errors were held to a minimum. The static pressure and the error in impact pressure were directly measured by visual observation of liquid-filled manometers. Liquids of different density were used in various ranges of pressure difference to permit large deflections at all times and thereby to reduce the effect of small accidental errors in the manometer readings. An estimate of the accidental error involved in the calibrations can be

obtained from the scatter of test points when the data are plotted. This scatter is approximately ±0.3 percent at low speeds and decreases at high speeds, where pressure differences are greater.

METHOD OF PRESENTATION

The results of the calibrations are presented in figures 6 to 22. The symbols used to designate the quantities measured are as follows:

p_i true impact pressure

p_s true static pressure

p_i' instrument impact pressure

p_s' instrument static pressure

In the calibration figures for each instrument, the error in static-pressure reading $\frac{p_s - p_s'}{p_i - p_s}$, the error in impact-pressure reading $\frac{p_i - p_i'}{p_i - p_s}$, and the calibration factor $\frac{p_i - p_s}{p_i' - p_s'}$ determined from the errors in static-pressure and impact-pressure readings are plotted against the indicated compression ratio $\frac{p_i' - p_s'}{p_s'}$, which is a function of the Mach number.

RESULTS AND DISCUSSION

Service Tubes

Tubes 1 a and 1 b.- Figure 6 shows that the static-pressure errors for tubes 1 a and 1 b are approximately constant though not equal over the greater part of the speed range. A comparison of the static-pressure errors for the two pitot-static tubes of this type shows that, in general, the error for tube 1 a is approximately twice

that for tube 1 b. The greater part of this difference may be due to surface irregularities in the vicinity of the static-pressure orifices of tube 1 b. On this instrument as delivered, the plating had been stripped a distance of two to four orifice diameters downstream from the orifices and a width of one orifice diameter behind each static-pressure orifice. (See plan view of tube in fig. 1.) The impact-pressure errors for the two tubes are approximately equal and are much smaller than the static-pressure errors. These small impact-pressure errors are caused by the presence of a bleed hole in the impact-pressure chamber, and they are to be expected in the use of any pitot-static tube having a bleed hole. The impact-pressure errors decrease slightly with increase in the indicated compression ratio. The impact-pressure errors and the static-pressure errors are in such directions that they are additive in the calibration factors. Inasmuch as the calibration factor is a combination of the two separate pressure errors, the explanation of the difference between the calibration factors for the two instruments is evident from the preceding discussion.

Tubes 2 a and 2 b.- Figure 7 shows that for tubes 2 a and 2 b the static-pressure errors are practically constant over the entire speed range. The static-pressure errors for the two tubes agree closely throughout the entire speed range; there is a practically constant difference of about 1/4 percent between the two.

The impact-pressure errors for the two tubes are equal and are numerically very small. There is a slight decrease in the impact-pressure errors with increasing velocities. The two pressure errors are additive in producing the calibration factors. The agreements between the calibration factors for the two instruments is close; the small difference is attributable to the difference in the static-pressure errors.

Tubes 3 a and 3 b.- Figure 8 shows that the static-pressure errors for tubes 3 a and 3 b are large and increase rapidly with increase in the indicated compression ratio. This rapid increase is the result of interference caused by the proximity of the mounting and pressure leads to the static-pressure orifices. The figure also shows that a decrease in the magnitude of the error, without change in the slope of the curve, occurs when a fairing is put over the part of the tube in contact with its main support. This result indicates that large interference

effects can be expected between the pitot-static tube and the surface on which it is mounted. The difference between the static-pressure errors for the two tubes is small in comparison with the total error.

The impact-pressure error for each of the tubes is zero. The explanation of the variation in the calibration factors (fig. 8(b)) is evident from the preceding discussion.

Prandtl Tube

Figure 9 shows that the error in static pressure for the Prandtl tube is small at low values of the indicated compression ratio, but it increases in magnitude as the indicated compression ratio is increased. This increase in error in the static-pressure reading with increasing speeds is exhibited by all the Prandtl-type pitot-static tubes that have been calibrated in the NACA 24-inch high-speed wind tunnel. The instrument of which the calibration is given here has been used as a standard tube against which others have been calibrated and has not been used in regular service. Consequently, the alinement of the portions ahead of and behind the static slot was more accurate than on any of the other Prandtl-type pitot-static tubes tested, and, as a result, the static-pressure error of this instrument was smaller than the errors of similar tubes calibrated. Figure 9 also shows that the impact-pressure error for the Prandtl-type pitot-static tube is negligible. The variation in the calibration factor is due to the variation in the static-pressure error.

High-Speed Tube

Figure 10 shows that the error in static-pressure reading for the high-speed pitot-static tube at $\alpha = 0^\circ$ is much smaller for nose A and nose B than for nose C and nose D. For noses A and B the static-pressure errors are very small, even for relatively high values of the indicated compression ratio. The static-pressure error for nose D is comparatively large at low speeds. This error is probably caused by one or a combination of the following factors: (1) separation of the flow about the nose; (2) the nearness of the static-pressure orifices to the region of maximum induced velocities about the nose, with the result that within this range the orifices are in a region of induced negative pressure.

Figure 11 shows that the impact-pressure error is negligible for all four nose shapes. Of the four calibration factors given in figure 12, the factors for noses A and B are nearer unity than the others. The calibration factors for noses A and B are practically equal to unity for all except the highest values of the indicated compression ratio.

Figure 13 shows that there is little change in the static-pressure errors for noses A, B, and C when the angle of attack is increased to 4°. The static-pressure error for nose D is comparatively large at an angle of attack of 4°. The impact-pressure errors for all the tubes at an angle of attack of 4° (fig. 14) differ appreciably from the values at 0° only for low values of the indicated compression ratio, at which the errors are of greater magnitude than at an angle of attack of 0°.

The calibration factors for the high-speed tube with different noses at 4° angle of attack are given in figure 15. The calibration factors for noses A and B are nearer unity than those for noses C and D. The calibration factor for nose B is nearer unity at low speeds but varies more from unity at high speeds than that for nose A.

The errors in static-pressure reading (fig. 16) for the high-speed tube with noses A, B, and C show a definite increase in magnitude at an angle of attack of 8°. Because of the large errors at angles of attack of 0° and 4° with nose D, calibrations with this nose shape were not made at angles of attack higher than 4°. The impact-pressure errors (fig. 17) also show a general increase in magnitude over the entire speed range. This increase in impact-pressure error is approximately equal for all the noses calibrated. The calibration factors shown in figure 18 differ considerably from those at small angles of attack. Inasmuch as the two separate pressure errors are in such directions that they cancel except at high values of the indicated compression ratio, the calibration factors at an angle of attack of 8° differ, except at the highest speeds, from those at an angle of attack of 0° by not more than $1\frac{1}{2}$ percent.

A further increase in the static-pressure errors, at an angle of attack of 12 , is shown in figure 19. The impact-pressure errors shown in figure 20 increase greatly at an angle of attack of 12°. As the two pressure errors

are in such directions that they tend to cancel in the calibration factors, the total errors, as shown by the calibration factors in figure 21, differ from the values for 0° angle of attack by 3 to 4 percent.

Comparison of Prandtl Tube and High-Speed Tube

The high-speed pitot-static tube was designed as a laboratory instrument and, as a result, its calibrations are directly comparable with those of other laboratory-type instruments. Figure 22 gives a comparison of the calibration factors for the Prandtl-type pitot-static tube and the high-speed pitot-static tube with nose A. At low speeds there is slight difference between the calibration factors for these two tubes. The factor for the Prandtl instrument, however, deviates from unity at a much lower speed than does the factor for the high-speed tube. At high speeds the calibration factor for the high-speed pitot-static tube is considerably nearer unity than is the calibration factor of the Prandtl-type instrument. Inasmuch as each of these instruments has a hemispherical nose, the better characteristics of the high-speed tube are evidently the result of: (1) a spindle shaped to give a smaller effect on the static pressure at the static-pressure orifices; (2) more accurate static-pressure indications with the small orifices than with the slot used on the Prandtl tube; and (3) a better location of the static-pressure orifices and support spindle for high speeds.

In the use of the calibration data the velocity can be determined in the following manner:

The abscissa of the calibration curves, the indicated compression ratio $\frac{p_i' - p_s'}{p_s'}$, can be determined from the instrument readings of the indicated impact pressure p_i' and the indicated static pressure p_s'. The calibration factor $\frac{p_i - p_s}{p_i' - p_s'}$ can be obtained from the figure presenting the calibration factor of the desired instrument. Then

$$p_i - p_s = \frac{p_i - p_s}{p_i' - p_s'} (p_i' - p_s')$$

The true impact pressure p_i and the true static pressure p_s can be determined by using either the impact-pressure error $\frac{p_i - p_i'}{p_i - p_s}$ or the static-pressure error $\frac{p_s - p_s'}{p_i - p_s}$ as obtained from the calibration curves. If the impact-pressure error is used, then

$$p_i - p_i' = \frac{p_i - p_i'}{p_i - p_s} (p_i - p_s)$$

$$p_i = (p_i - p_i') + p_i'$$

and

$$p_s = p_i - (p_i - p_s)$$

The velocity V can be obtained from the relation

$$V^2 = \frac{2\rho\gamma}{\gamma - 1} \frac{p_s}{\rho_s} \left[\left(\frac{p_i}{p_s} \right)^{\frac{\gamma-1}{\gamma}} - 1 \right]$$

where

γ ratio of specific heat at constant pressure to specific heat at constant volume (taken as 1.40 for air)

ρ_s mass density of air static pressure p_s and ambient-air temperature

CONCLUSIONS

Calibrations of three types of service and two types of laboratory pitot-static tubes, made over an approximate range of speeds of 150 to 600 miles per hour, indicate the following conclusions:

1. The calibrations of the Kollsman Instrument Co. F.S.S.C. No. 18-T-4545-type pitot-static tubes and the Aero Instrument Co. F.S.S.C. No. 18-T-4554-type pitot-static tubes indicated that the pressure errors for each of these types of instrument are comparatively small and are approximately constant over a large speed range.

2. The Aero Instrument Co. N.A.F. 39968-type pitot-static tube showed large interference effects between the tube and the surface on which it was mounted. This interference was so great that the use of this type of instrument would probably be undesirable.

3. The difference in the calibrations of the two Kollsman Instrument Co. F.S.S.C. No. 18-T-4545 pitot-static tubes, inasmuch as the only difference in the instruments was the presence of surface irregularities near the static-pressure orifices of one instrument, indicated the importance of having a smooth surface in the region of the static-pressure orifices in order to obtain accurate results.

4. The standard Prandtl-type pitot-static tube and the high-speed pitot-static tube with hemispherical and 2:1 semiellipsoidal nose shapes were found to have similar calibrations at low speeds but at high speeds the high-speed tubes were found to have better characteristics than the Prandtl-type tube. The high-speed pitot-static tube with hemispherical and 2:1 semiellipsoidal nose shapes had practically constant calibration factors at values of the Mach number from 0.2 to 0.7. Throughout this speed range the calibration factor for each of these tubes was 1.000 $\pm$0.002 at an angle of attack of 0°. Throughout the same speed range and at angles of attack as high as 8°, the greatest error introduced was not greater than $1\frac{1}{2}$ percent for either nose shape.

5. Although designed as a laboratory instrument, the high-speed pitot-static tube, with small modifications that should introduce only a small change in the total error of the instrument, may be suitable for service use.

Langley Memorial Aeronautical Laboratory,
National Advisory Committee for Aeronautics,
Langley Field, Va.

REFERENCES

1. Stack, John, Lindsey, W.F., and Littell, Robert E.: The Compressibility Burble and the Effect of Compressibility on Pressures and Forces Acting on an Airfoil. Rep. No. 646, NACA, 1938.

2. Walchner, O.: The Effect of Compressibility on the Pressure Reading of a Prandtl Pitot Tube at Subsonic Flow Velocity. T.M. No. 917, NACA, 1939.

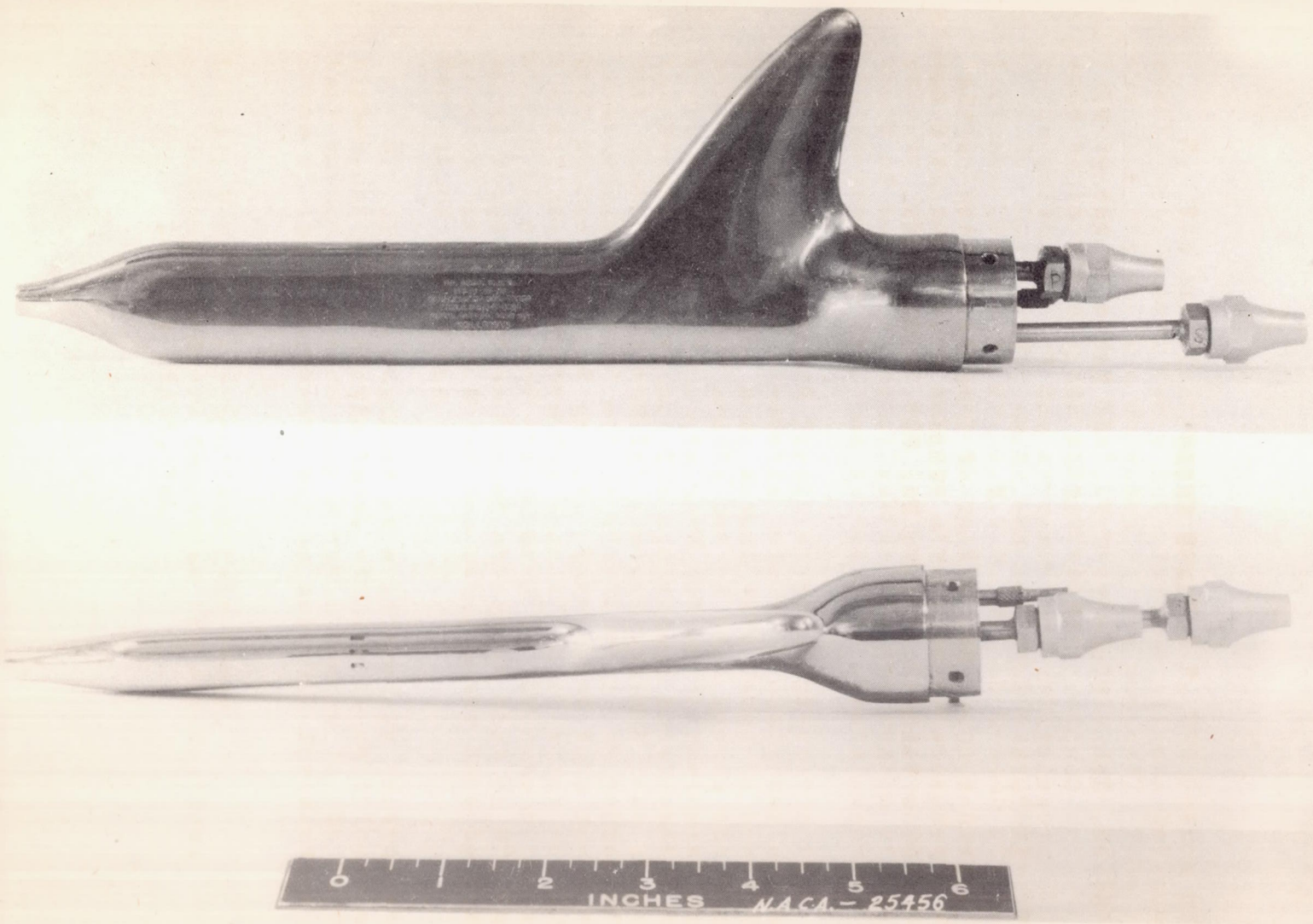

Figure 1.- Kollsman Instrument Co., F.S.S.C. No. 18-T-4545 pitot-static tube; tubes 1 a and 1 b .

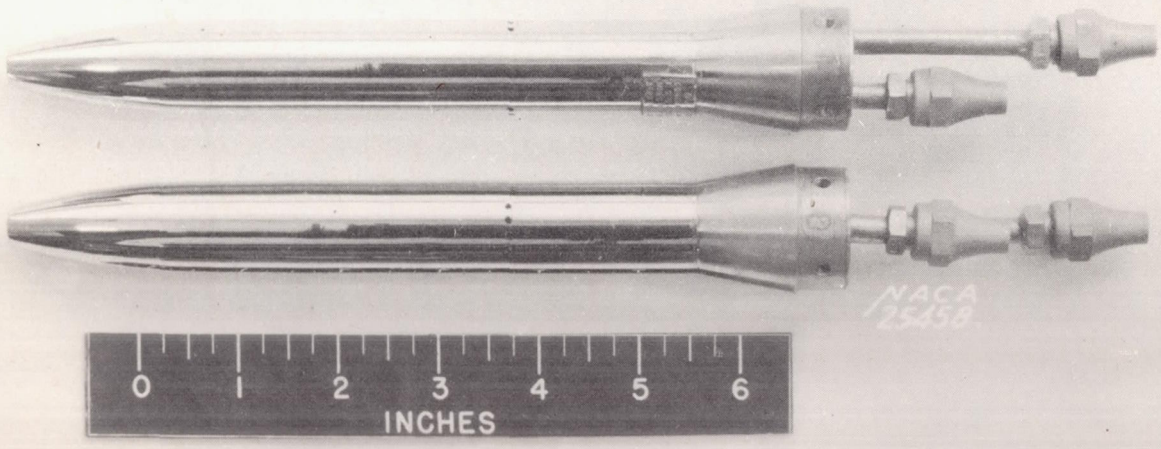

Figure 2.- Aero Instrument Co., F.S.S.C. No. 18-T-4554 pitot-static tube; tubes 2a and 2b.

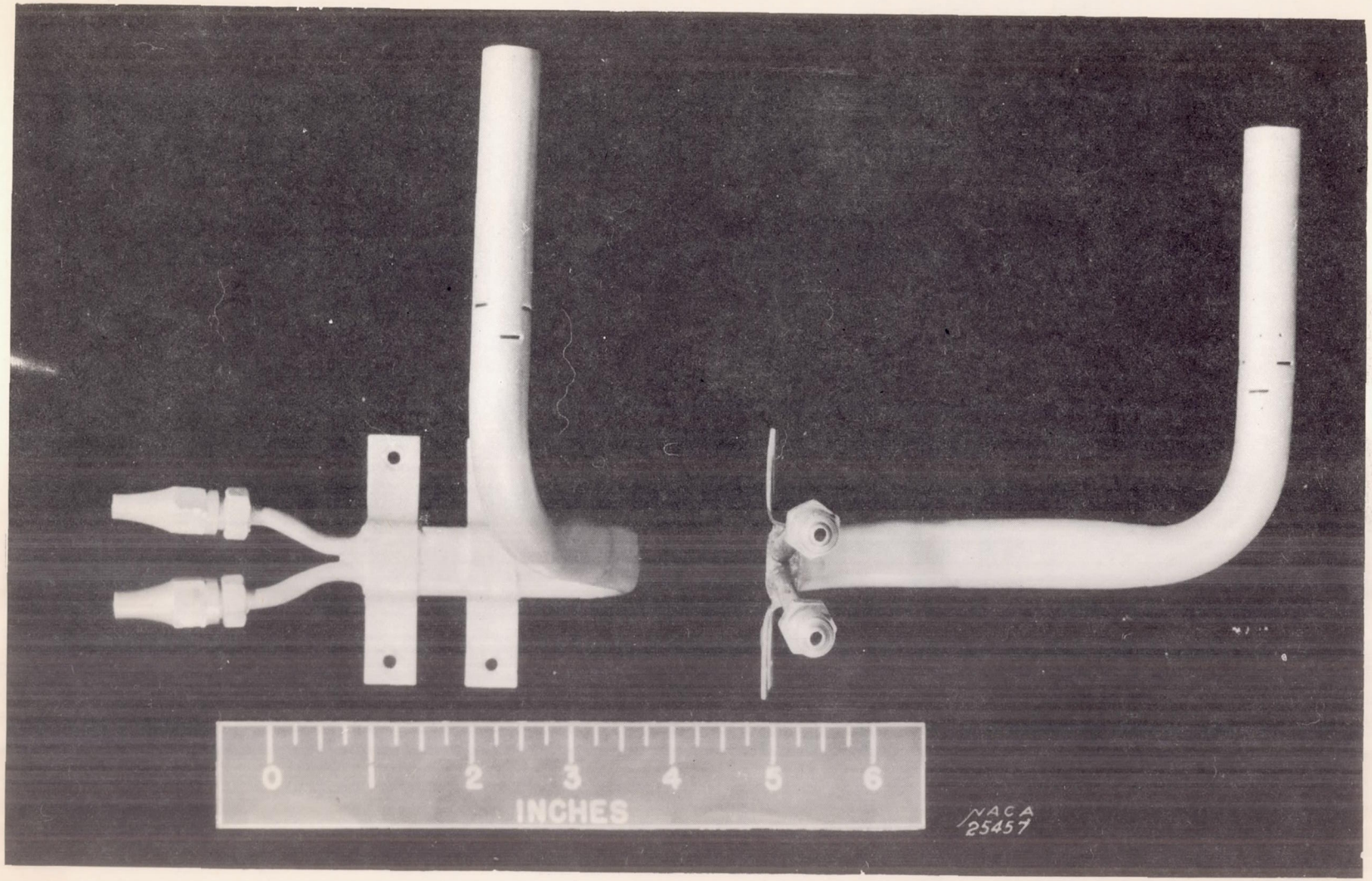

Figure 3.- Aero Instrument Co., N.A.F. 39968. Bureau of Aeronautics drawing No. 548-SK pitot-static tube; tubes 3a and 3b.

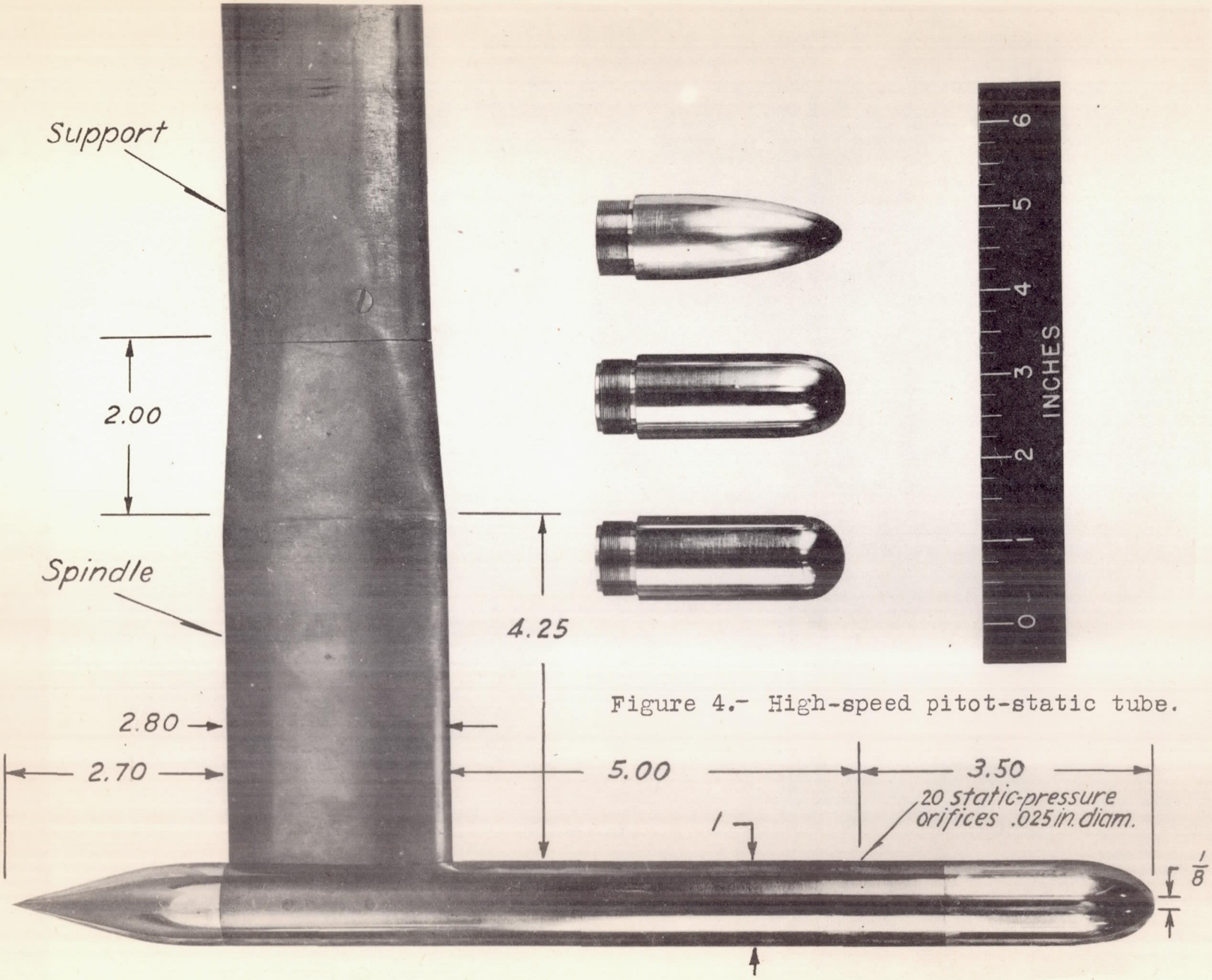

Figure 4.- High-speed pitot-static tube.

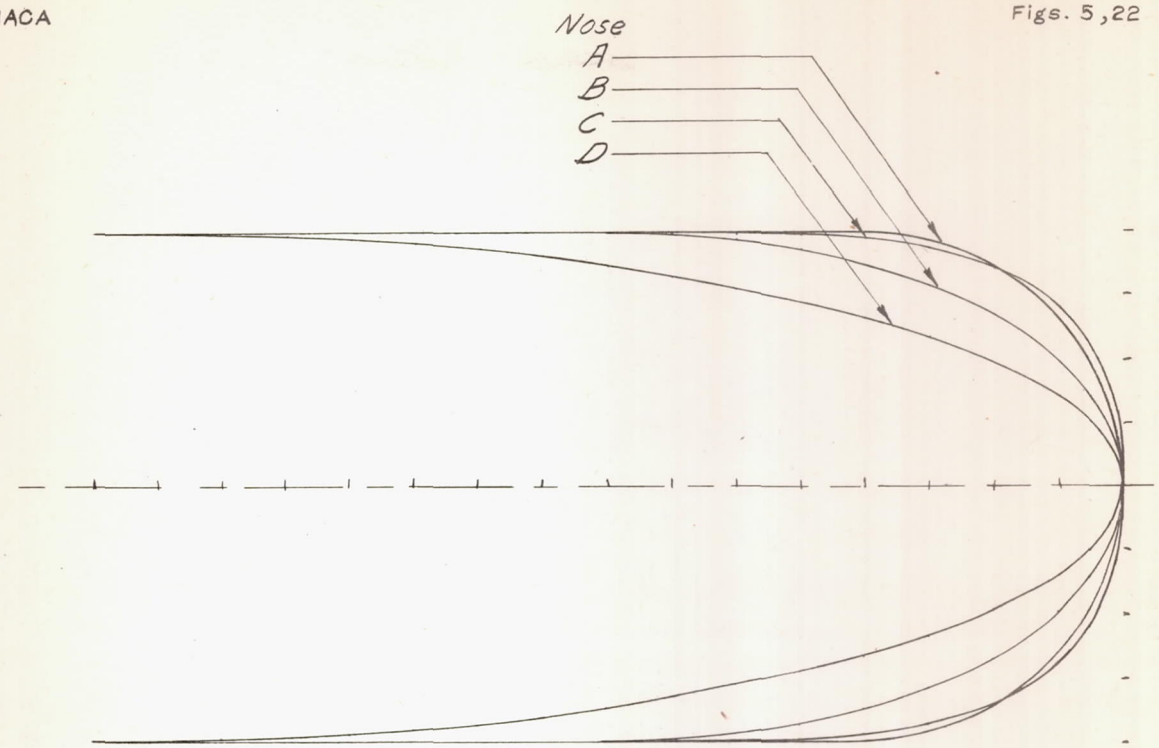

Figure 5.- Comparison of four nose shapes tested on the high-speed pitot-static tube.

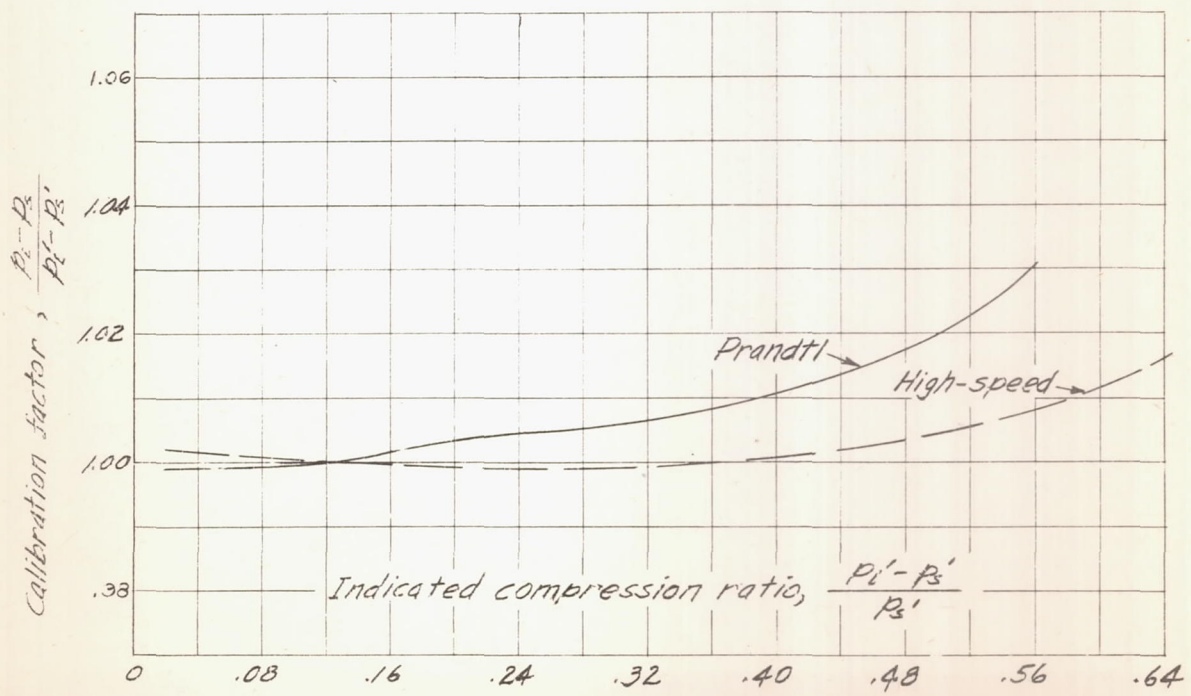

Figure 22.- Comparison of the calibration factors for the standard Prandtl type pitot-static tube and the high-speed pitot-static tube with hemispherical nose. $\alpha=0^{\circ}$.

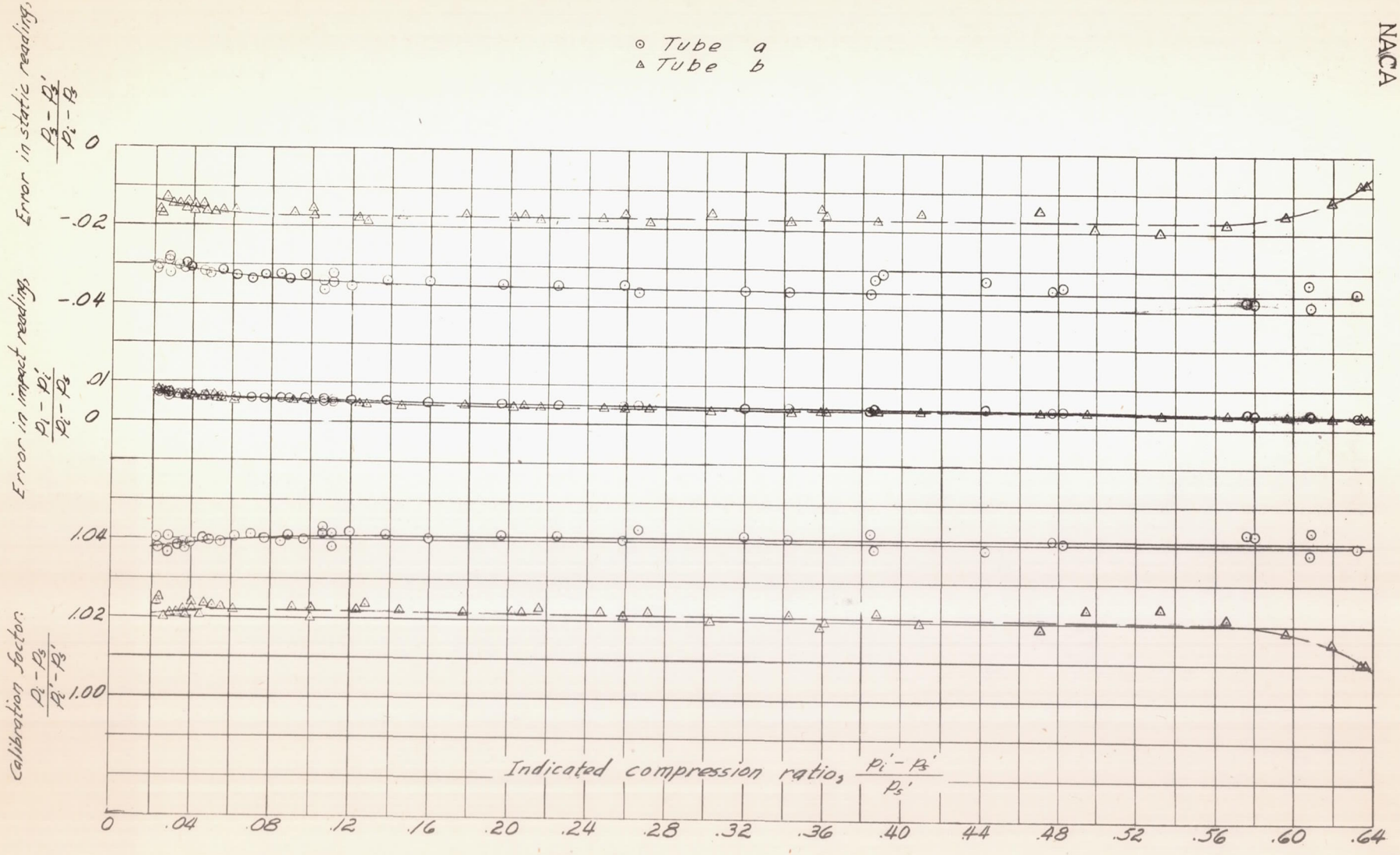

Figure 6.— Calibration for tubes 1a and 1b. $\alpha = 0°$.

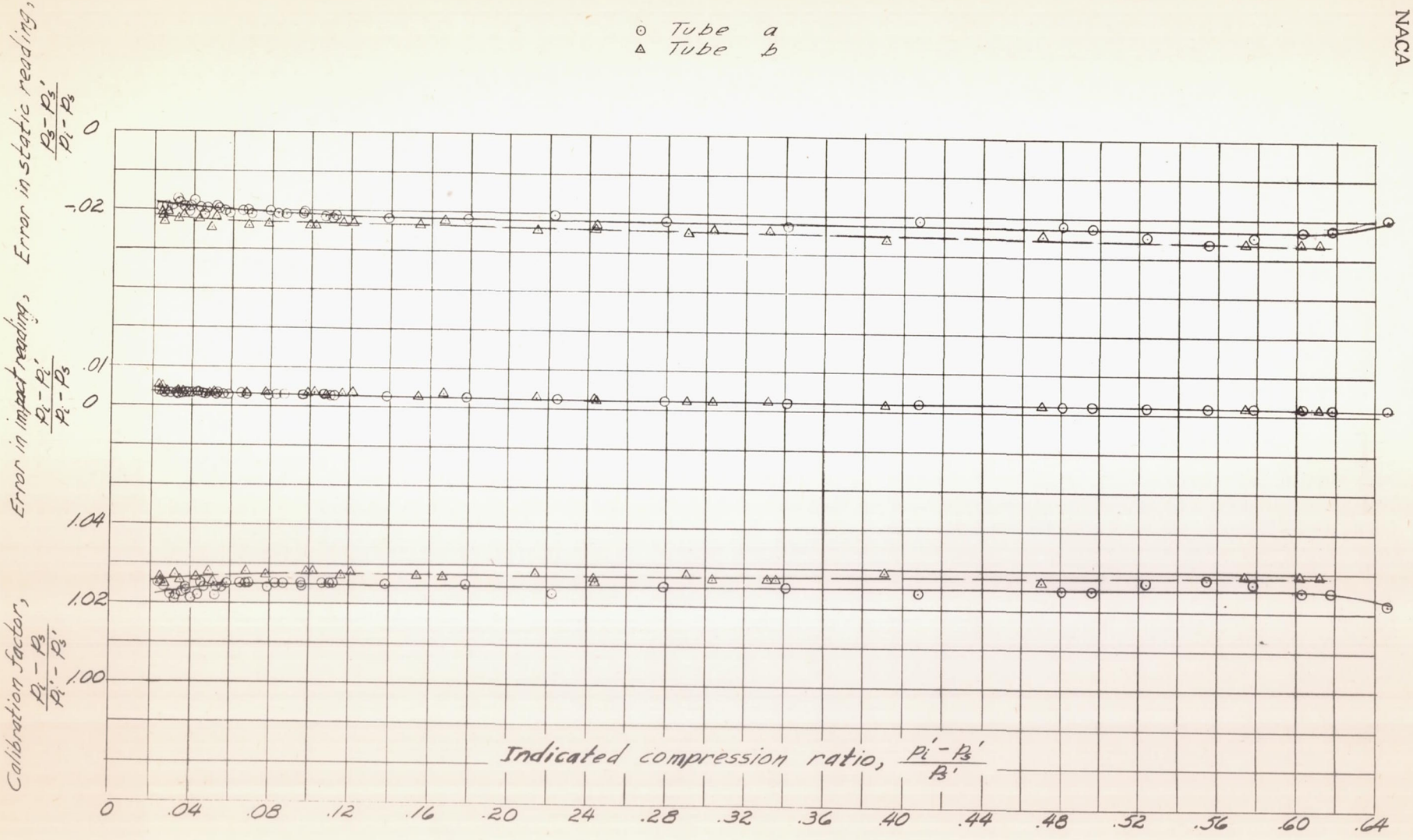

Figure 7.— Calibration for tubes 2 a and 2 b. $\alpha = 0°$

NACA

Fig 7

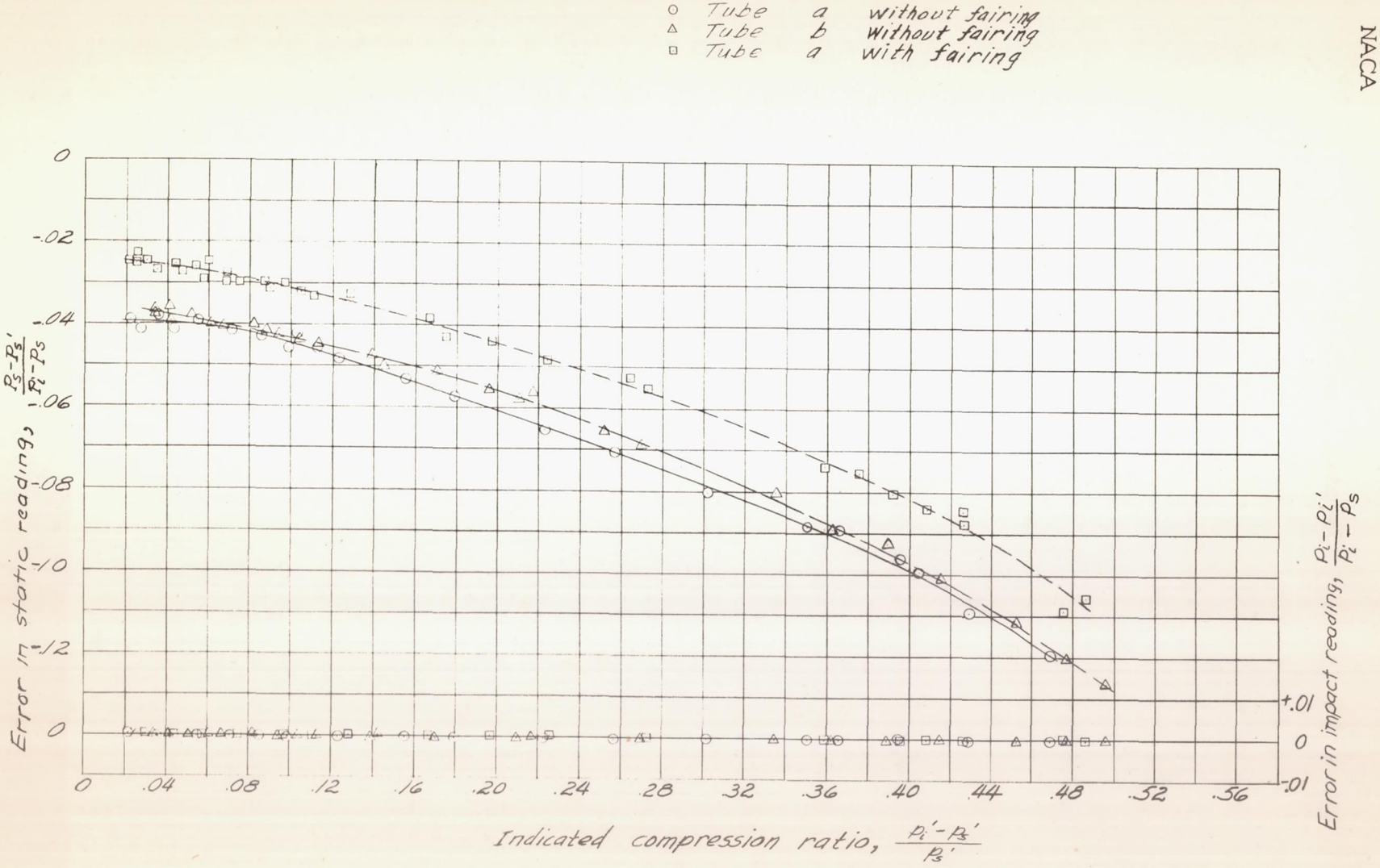

(a) Pressure errors.

Figure 3.— Calibration for tubes 3 a and 3 b. $\alpha = 0°$.

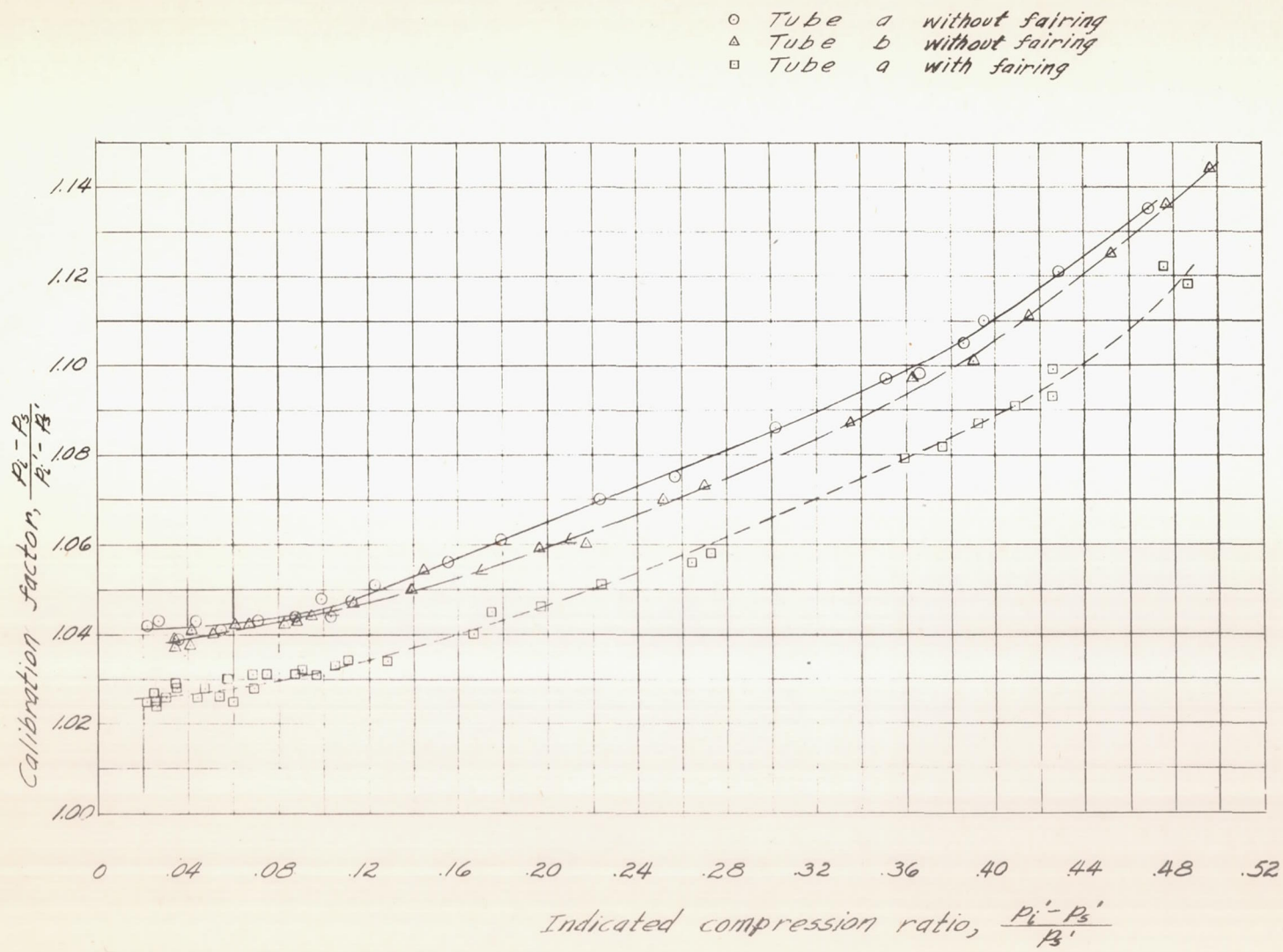

Fig. 8b

Figure 8.- Concluded. (b) Calibration factor.

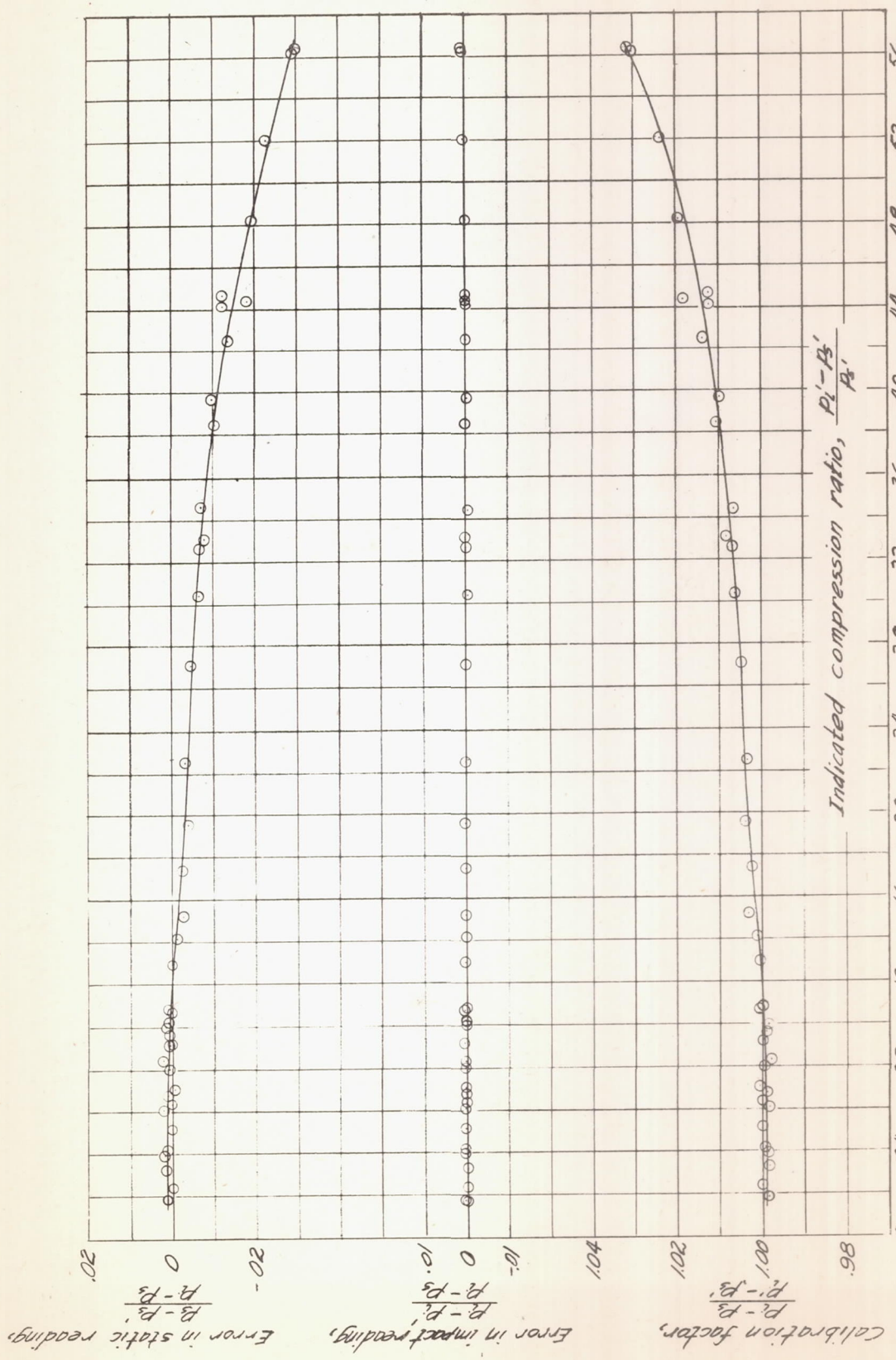

Figure 9.- Calibration for standard Prandtl type pitot-static tube. $\alpha = 0°$.

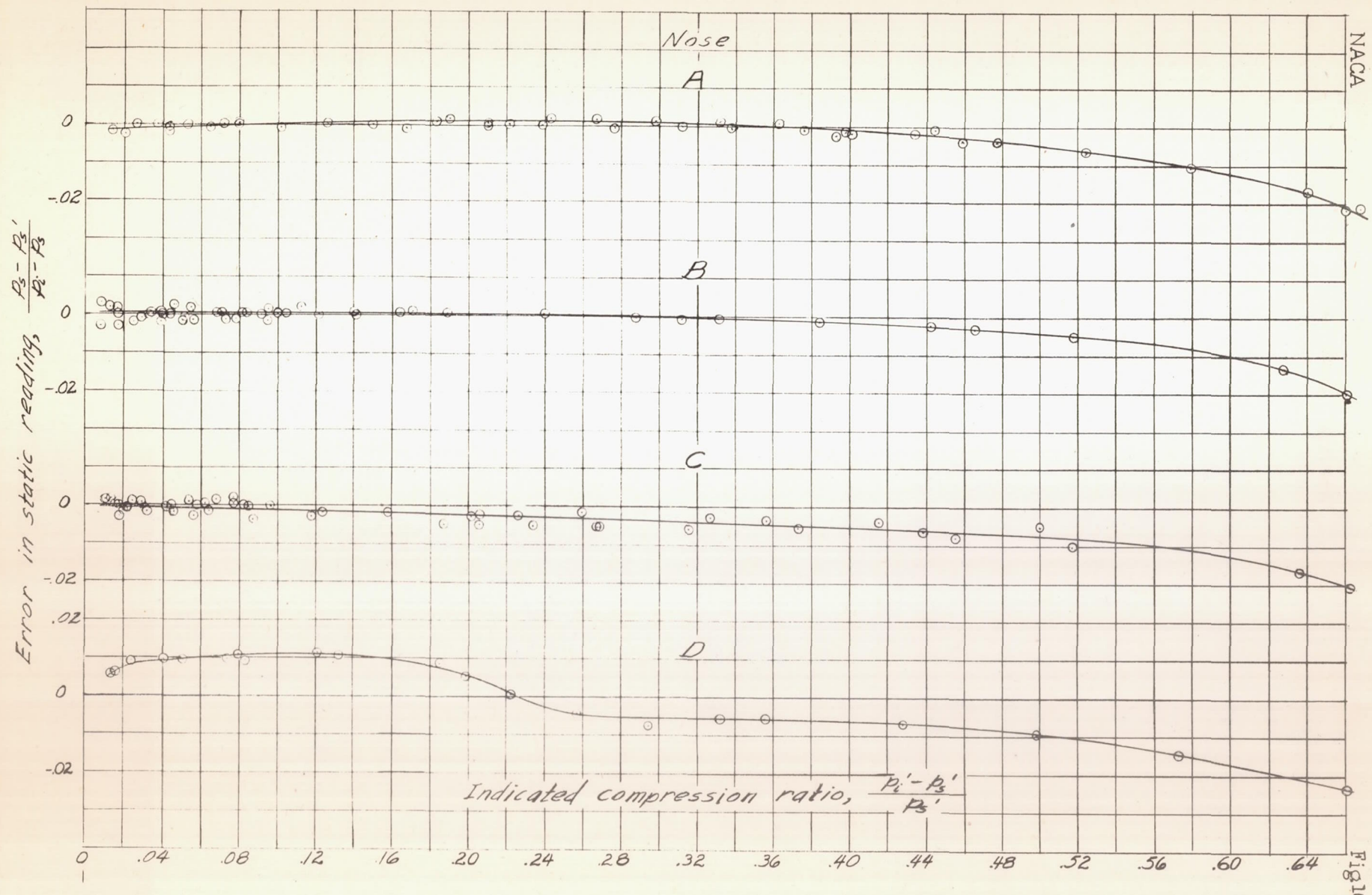

Figure 10.- Error in static-pressure reading for the high-speed pitot-static tube. $\alpha = 0.°$

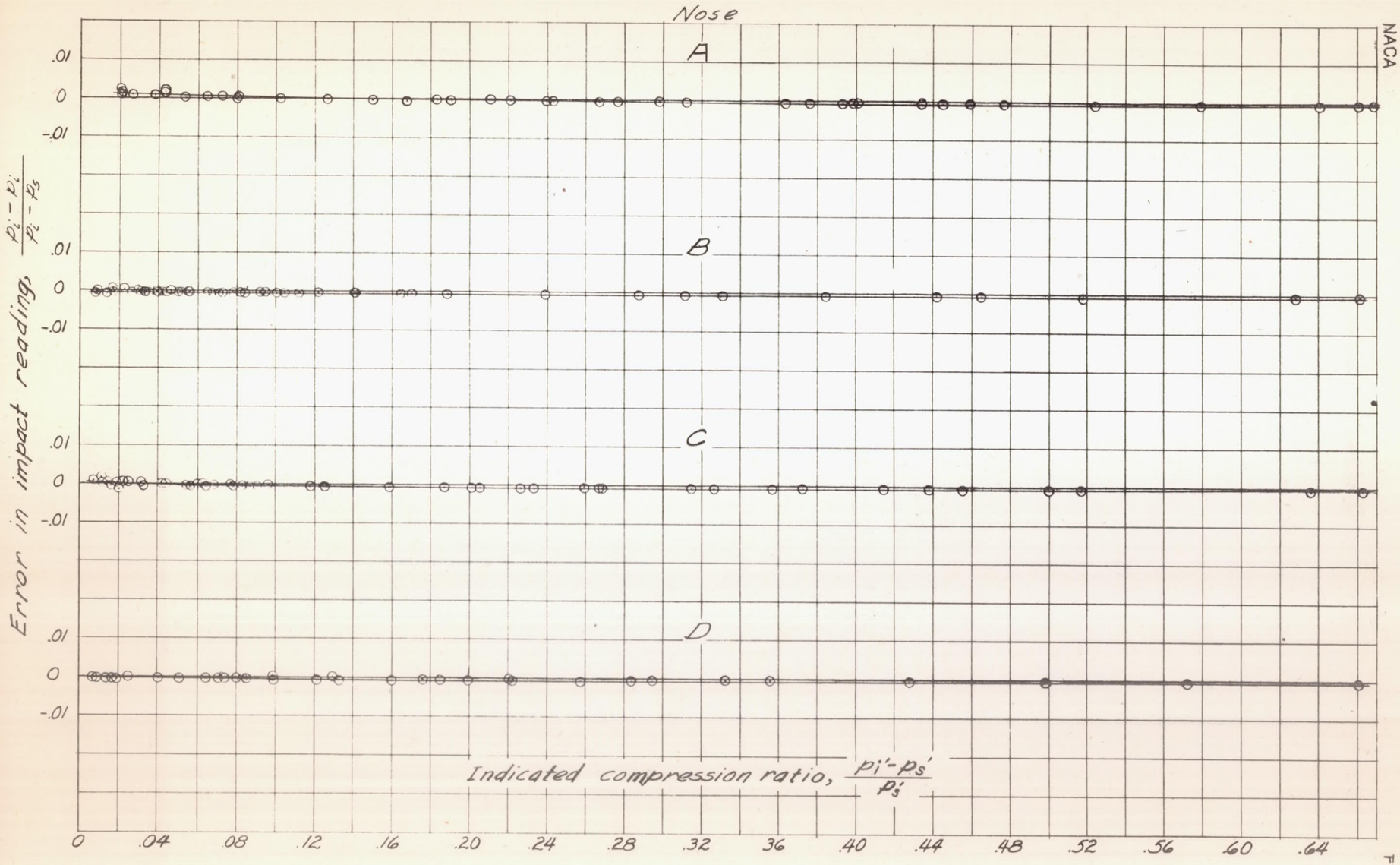

Figure 11.– Error in impact-pressure reading for the high-speed pitot-static tube. $\alpha = 0°$.

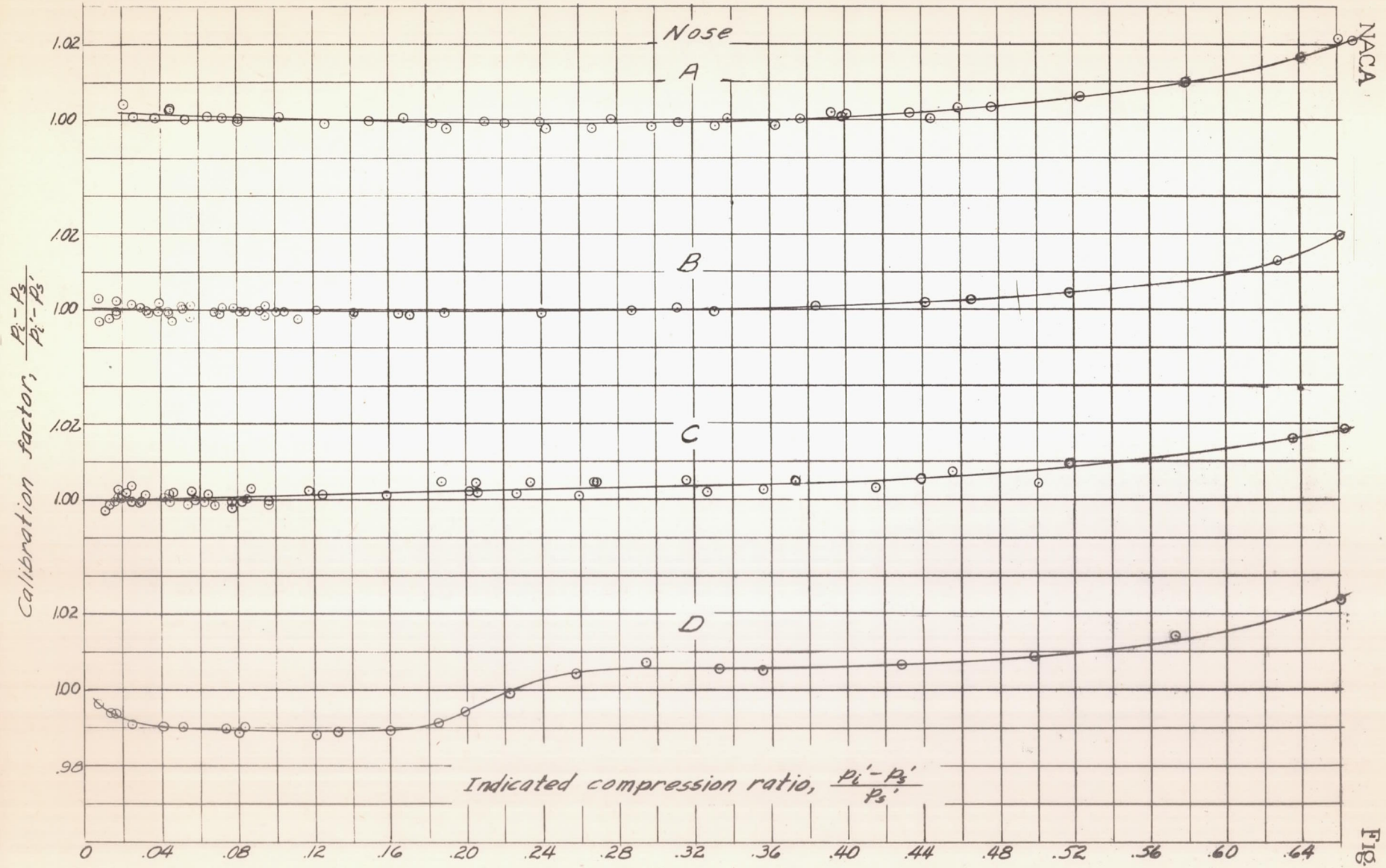

Figure 12.- Calibration factor for the high-speed pitot-static tube. $\alpha = 0°$.

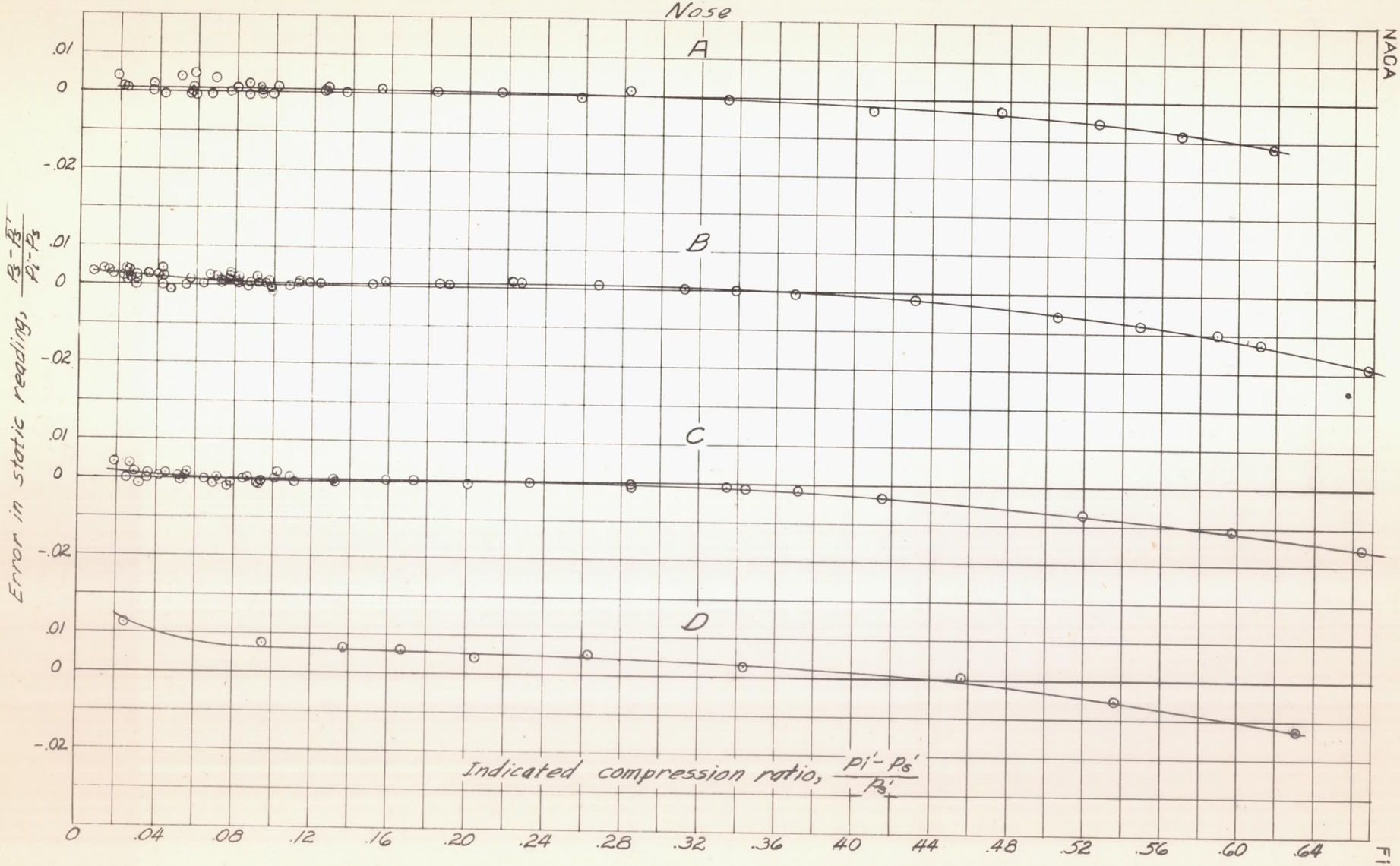

Figure 13.- Error in static-pressure reading for the high-speed pitot-static tube. $\alpha = 4°$.

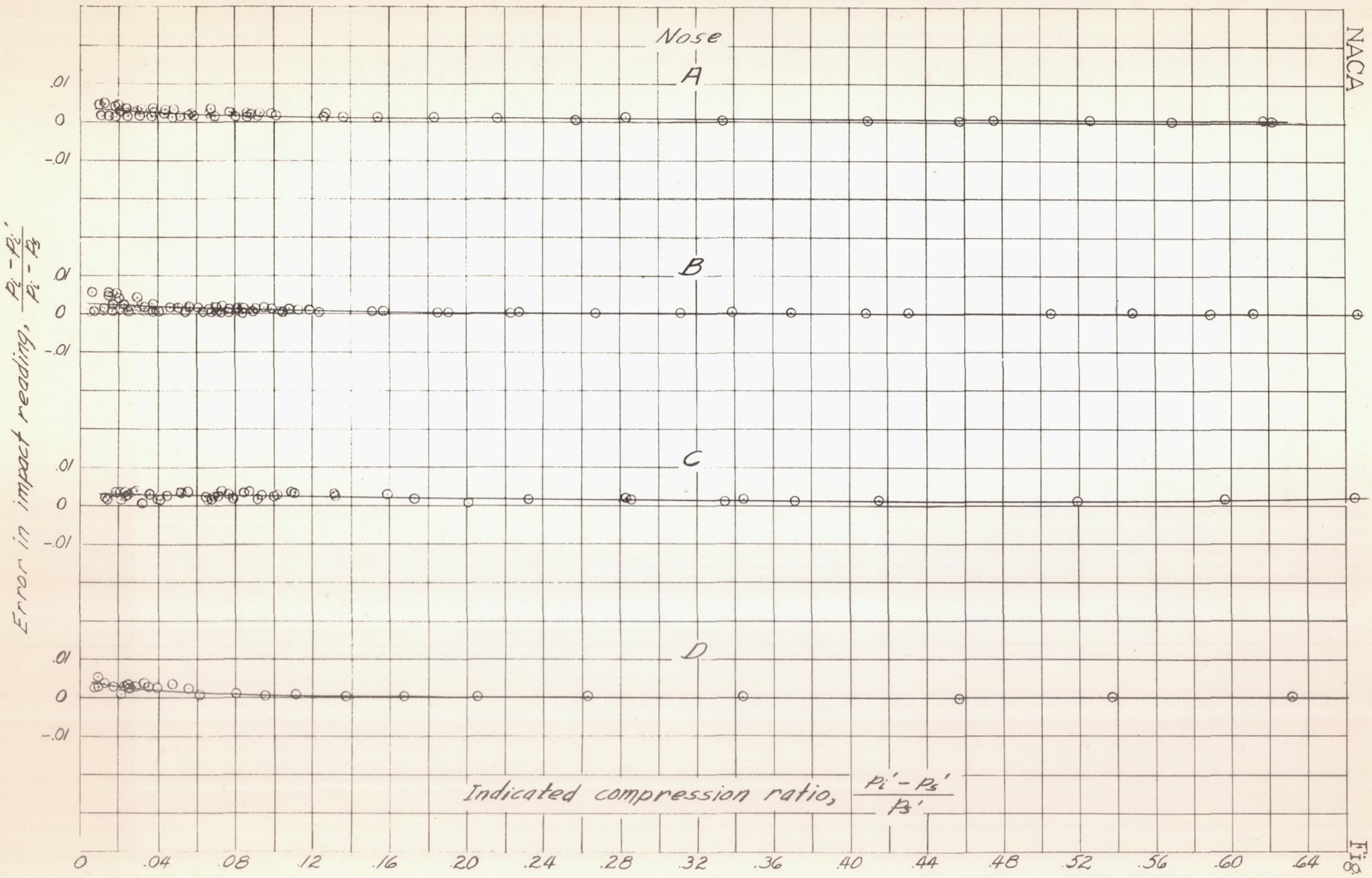

Figure 14. - Error in impact-pressure reading for the high-speed pitot-static tube. $\alpha = 4°$.

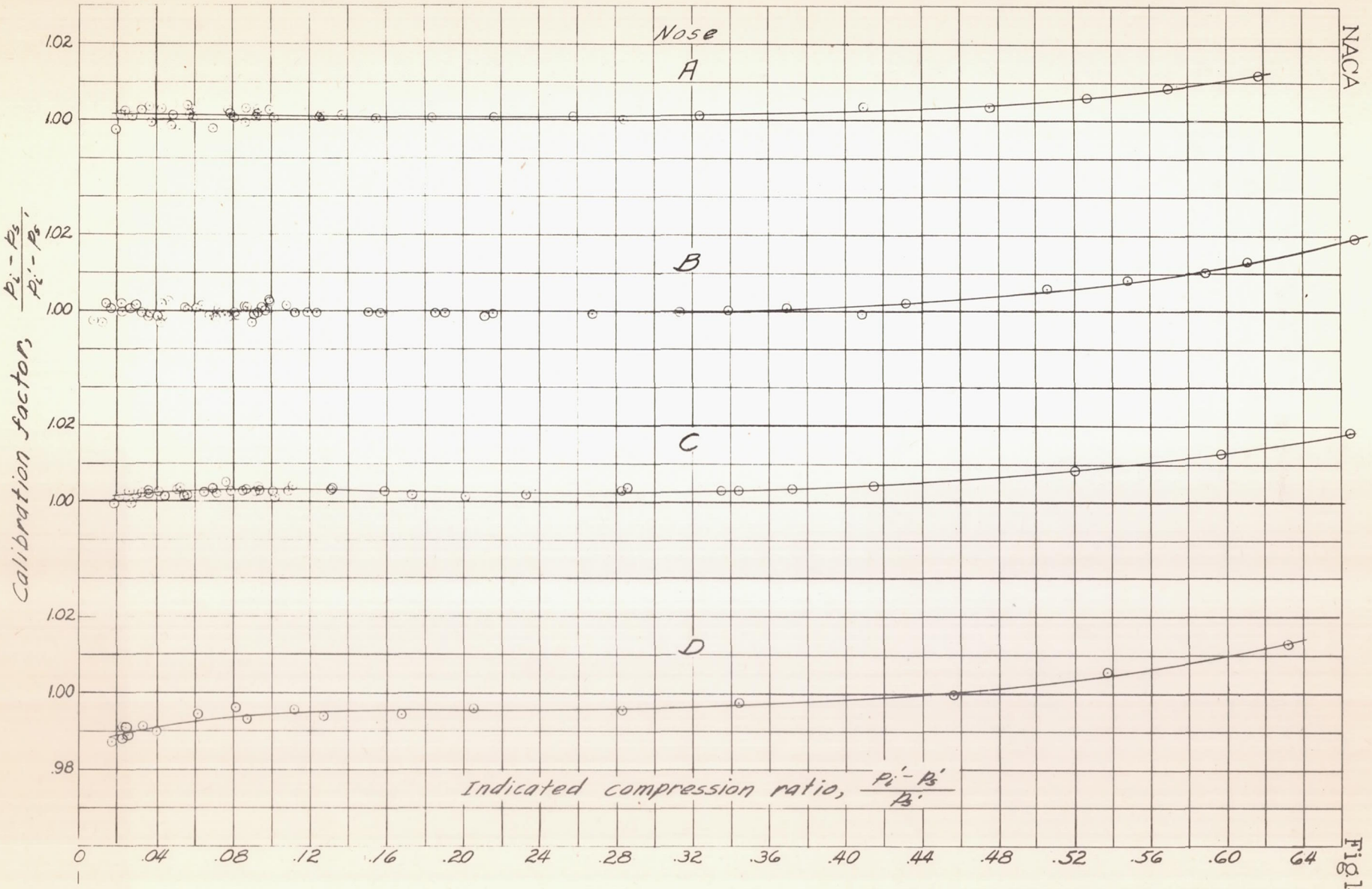

Figure 15.— Calibration factor for the high-speed pitot-static tube. $\alpha = 4°$.

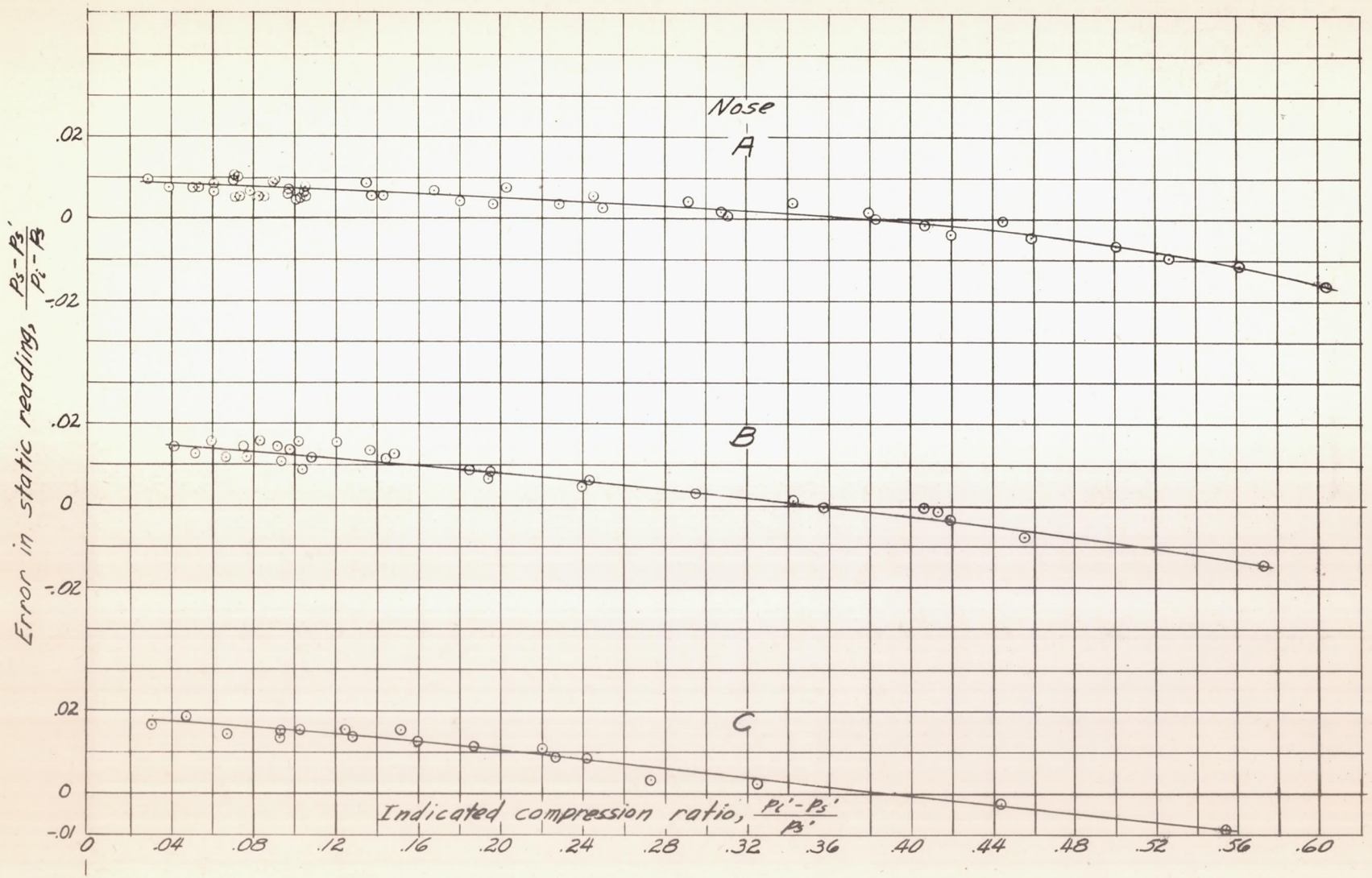

Figure 16.– Error in static-pressure reading for the high-speed pitot-static tube. $\alpha = 8°$.

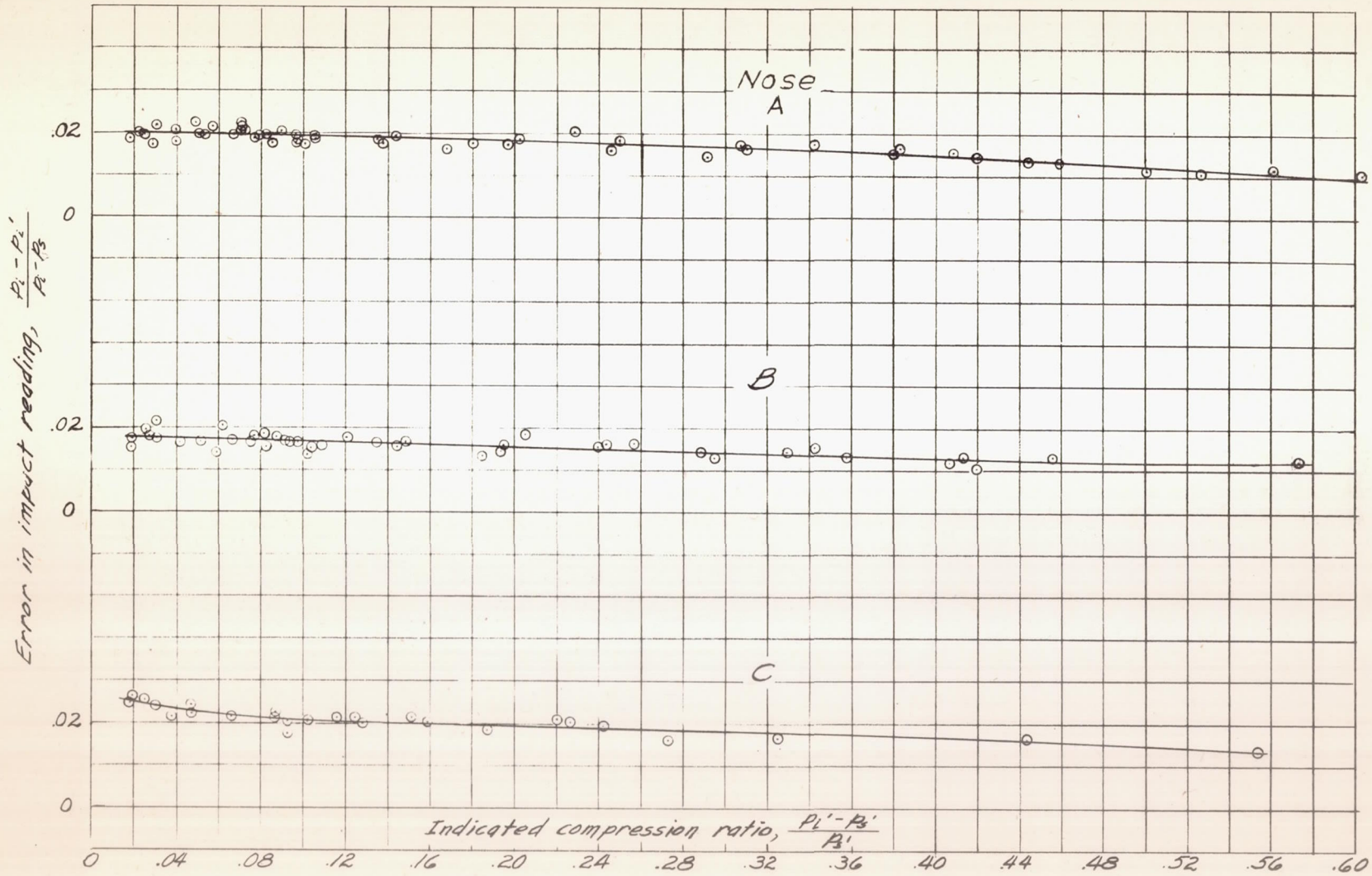

Figure 17.- Error in impact-pressure reading for the high-speed pitot-static tube $\alpha = 8°$.

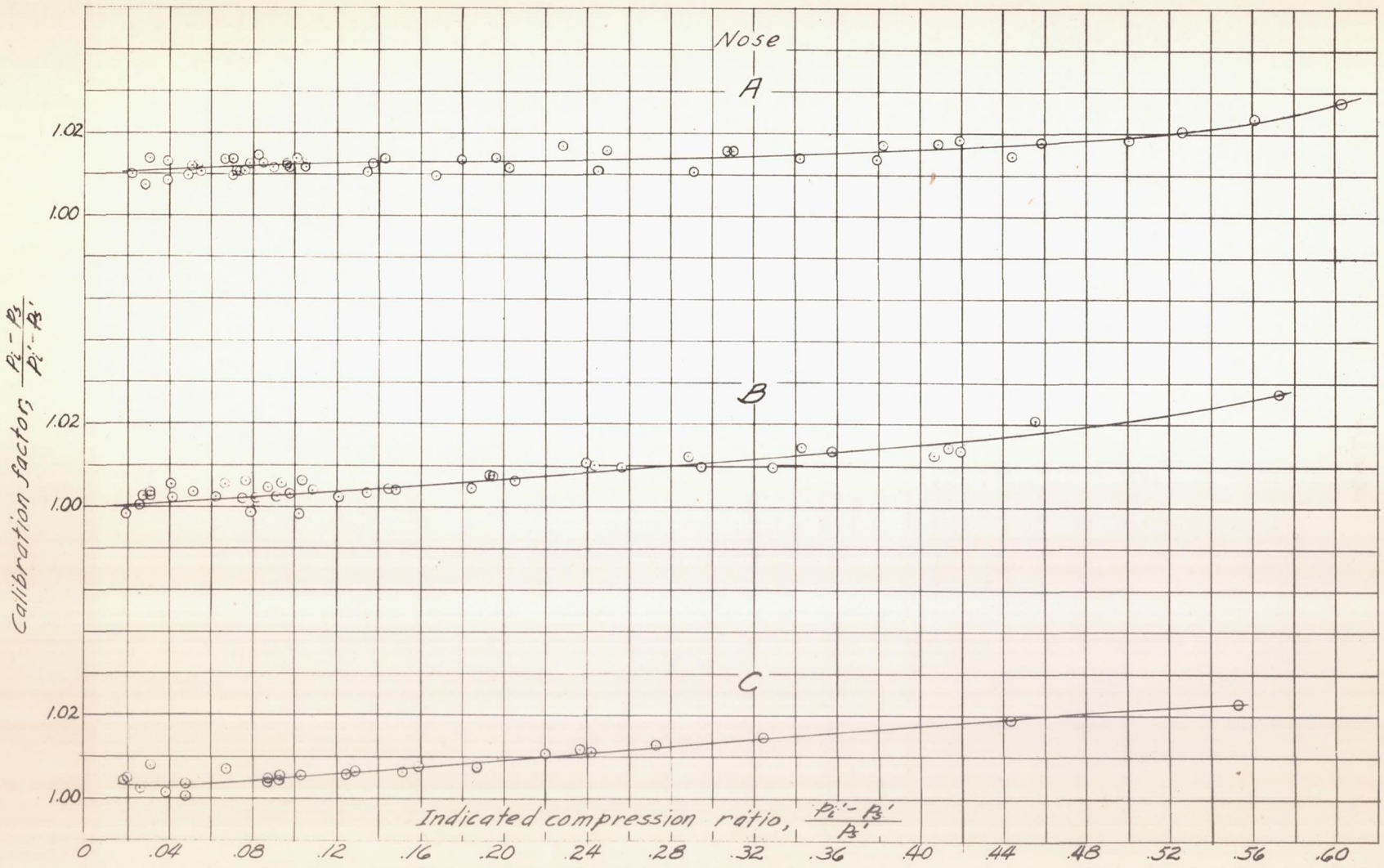

Figure 18. – Calibration factor for the high-speed pitot-static tube. $\alpha = 8°$.

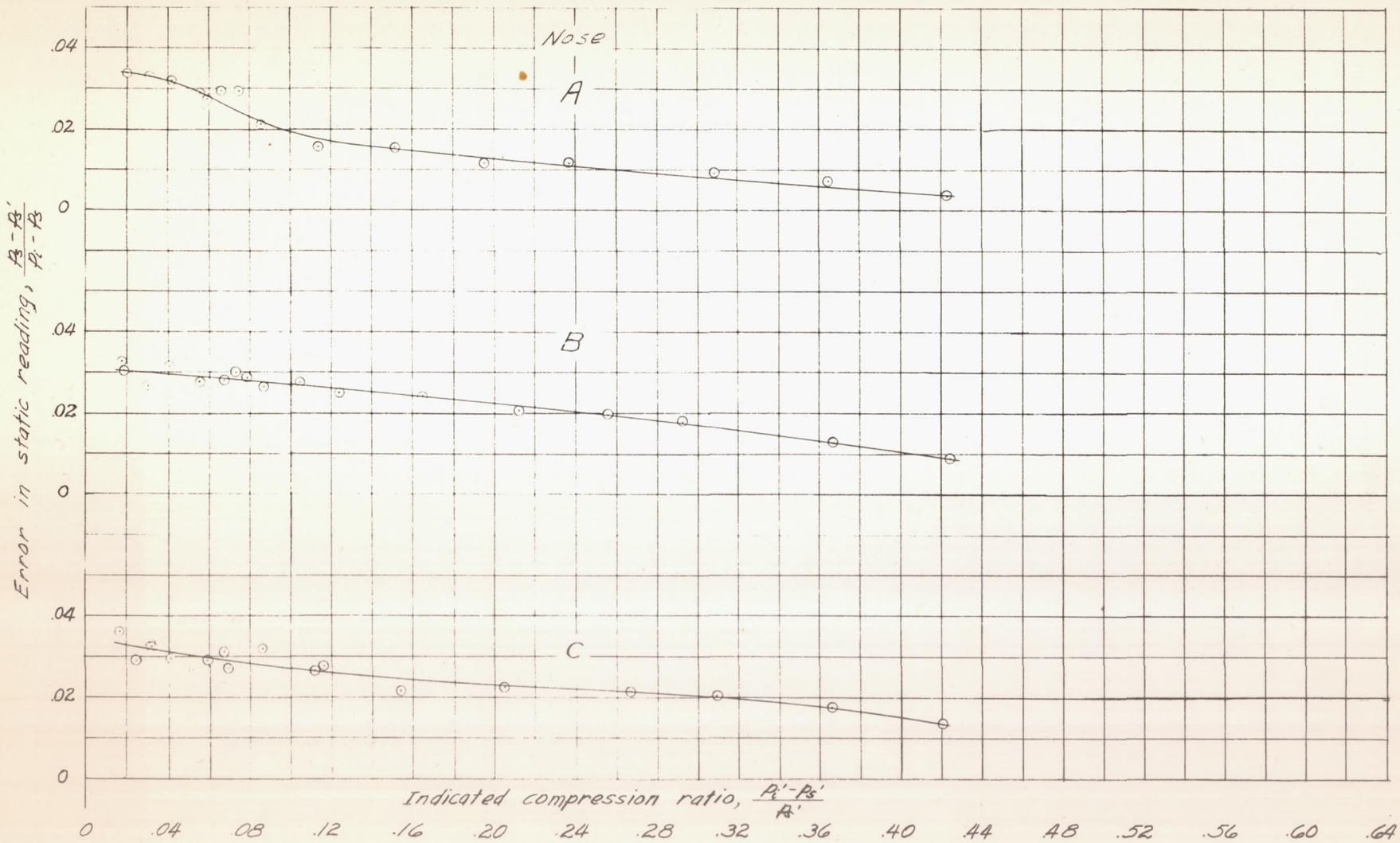

Figure 19. — Error in static-pressure reading for the high-speed pitot-static tube. $\alpha = 12°$.

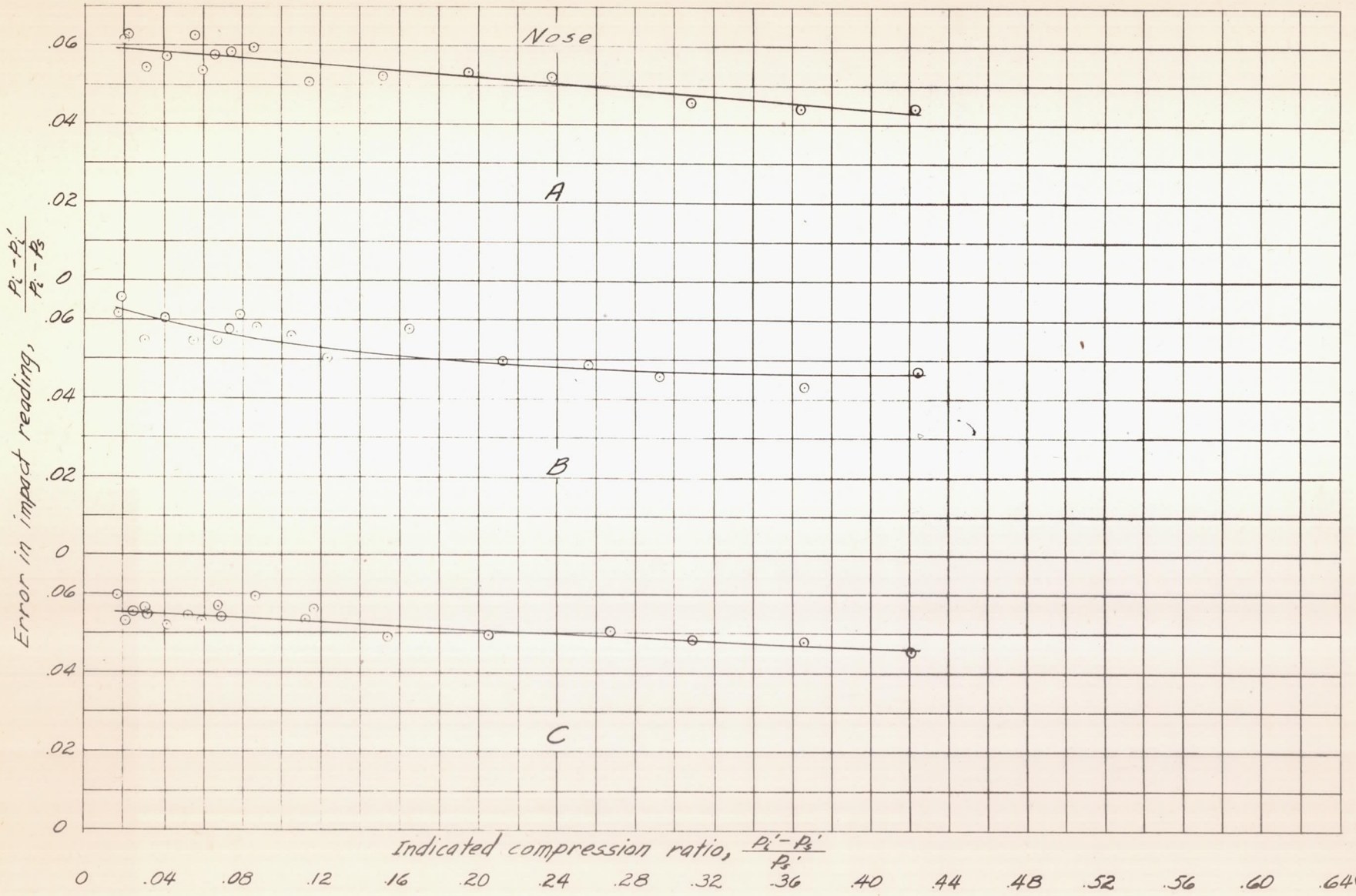

NACA

Fig 20

Figure 20.— Error in impact-pressure reading for the high-speed pitot-static tube. $\alpha = 12°$.

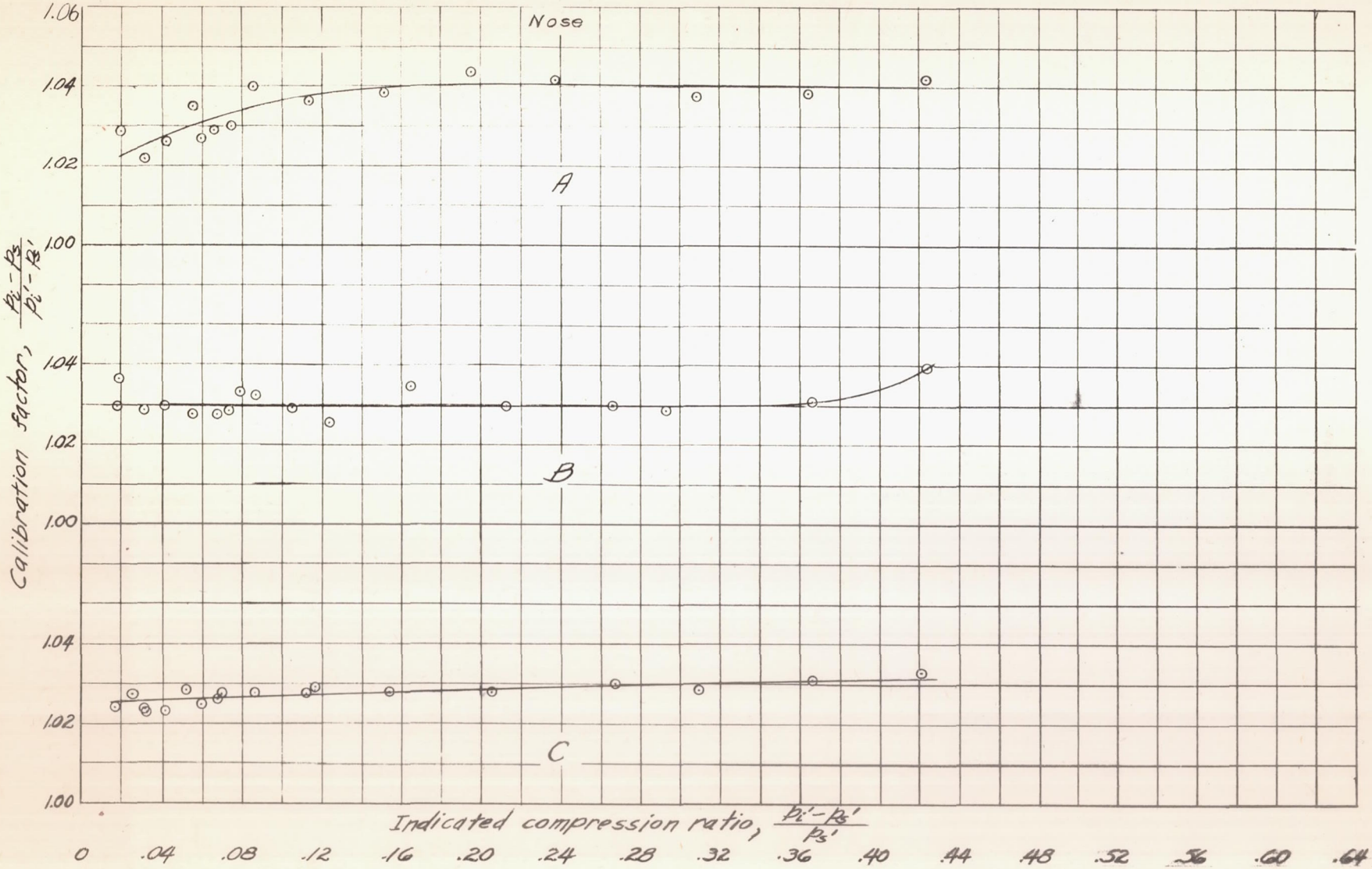

NACA

Fig. 21

Figure 21.- Calibration factor for the high-speed pitot-static tube. $\alpha = 12°$